

## Full Length Article

# On the self-heating behavior of upgraded biochar pellets blended with pyrolysis oil: Effects of process parameters

Lorenzo Riva<sup>a,\*</sup>, Alessandro Cardarelli<sup>b</sup>, Geir Johan Andersen<sup>c</sup>, Therese Videm Buø<sup>c</sup>, Marco Barbanera<sup>b</sup>, Pietro Bartocci<sup>d</sup>, Francesco Fantozzi<sup>d</sup>, Henrik Kofoed Nielsen<sup>a</sup>

<sup>a</sup> Department of Engineering Sciences, University of Agder, Postboks 509, 4898 Grimstad, Norway

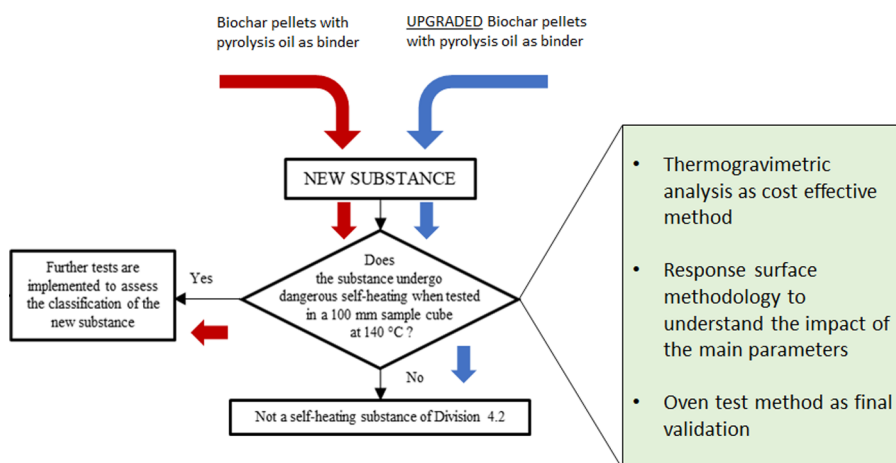
<sup>b</sup> Department of Economics, Engineering, Society and Business Organization, University of Tuscia, 01100 Viterbo, Italy

<sup>c</sup> Elkem AS, Fiskåveien 10, 4621 Kristiansand, Norway

<sup>d</sup> Department of Engineering, University of Perugia, Via G. Duranti 67, 06125 Perugia, Italy



## GRAPHICAL ABSTRACT



## ARTICLE INFO

## Keywords:

Densification

Pellet

Self-heating

Biochar

Pyrolysis oil

Response surface methodology

## ABSTRACT

Biochar obtained from biomass pyrolysis is a promising carbon neutral material which can be used in substitution of fossil coal and coke in metallurgical applications. Biochar's mechanical properties improve significantly without compromising reactivity, when upgraded by densification with pyrolysis oil and reheated. However, upgraded biochar pellets use in the industry is limited due to the risks associated with self-heating. This issue must be seriously considered for further industrial production of upgraded biochar pellets. Self-heating oven tests are generally time-consuming and limit the possibility of testing various potential solutions. The aim of this work was both to investigate the self-heating behavior of densified biochar and to possibly substitute the standard oven test with a fast and cost-effective thermogravimetric analysis. This was done by using Response Surface Methodology, where pyrolysis temperature, oil content and treatment temperature were selected as independent variables. By statistical analysis it was possible to understand that self-heating risk can be drastically reduced by upgrading the pellets at high temperatures (i.e. re-heating). In addition, through the analysis of the initial combustion temperature, the maximum weight loss rate and the activation energy

\* Corresponding author.

E-mail address: [lorenzo.riva@uia.no](mailto:lorenzo.riva@uia.no) (L. Riva).

<https://doi.org/10.1016/j.fuel.2020.118395>

Received 27 February 2020; Received in revised form 14 May 2020; Accepted 11 June 2020

Available online 19 June 2020

0016-2361/ © 2020 The Authors. Published by Elsevier Ltd. This is an open access article under the CC BY license

(<http://creativecommons.org/licenses/by/4.0/>).

(considered as responses of the model), it was possible to understand how to predict the results of the self-heating oven tests through thermogravimetric analysis.

## 1. Introduction

Greenhouse Gases (GHG) should be reduced implementing not a single but many possible sustainable solutions [1]. Due its carbonaceous nature, biochar might efficiently be applied in industries which are typically dependent on fossil coal and coke [2]. A specific sector, where biochar has been largely considered as a promising solution, is the metallurgical industry [3–8]. Unfortunately, the metallurgical application of biochar is limited by the uncompetitive price (in comparison to coal and coke) and insufficient mechanical characteristics [9]. The latter issue results in challenges both in handling, transportation, storage with a consequent increase of costs, due to mass losses [10]. There are problems also in the smelting furnace, where strong and stable materials are appreciated [8]. A solution has been suggested and investigated in [11], where biochar was densified using pyrolysis oil as binder and the produced pellets were newly pyrolyzed (re-heated). The process improved considerably density, mechanical durability and compressive strength of the biochar, without compromising fixed carbon content and reactivity, which are fundamental properties requested by the industry [12]. The same solution was further developed at an industrial scale in [13]. Recently, the industrial production of thermally treated biochar pellets with pyrolysis oil has been further investigated. However, it is still not very clear how densification and addition of pyrolysis oil may increase the risk of self-heating, which is the tendency of certain porous fuels to undergo spontaneous exothermic reactions, in absence of any external ignition, at relatively low temperatures and in an oxidative atmosphere [14]. When the heat generated cannot be entirely dispersed, the temperature increases, potentially leading to ignition [15,16]. Since the heat generation is related to the volume, while the heat losses to the surface, the risk increases when the material is stored in large piles, limiting the possibility to transport and store large volumes [17]. A test method evaluating self-heating risk is already available, and it is based on the combustion theory and empirical observations [18,19]. The method is based on heating the sample in an isothermal oven test, where volumes, temperatures and test times are fixed. Using this test it is possible to scale up the results to larger volumes and understand if a material can be stored and shipped safely [20]. This methodology can be followed by applying either the standard test EN 15,188 or the UN IMO test N.4 [21]. This kind of test has been used for several biomasses [20,22,23]. It was also applied to biochar in [15,21]. In particular, it was observed in [15], that the pyrolysis temperature has a strong impact on the self-heating behavior of biochar and, when the biomass is pyrolyzed at 450 °C, the resulting biochar has a relatively high risk of igniting. The standard oven tests, however, necessitate of a considerable amount of material and their completion requires generally 24 h. Other faster methods have been hence studied and applied [15]. For its simplicity and low demand in term of material and time, thermal analysis has been deeply studied as a feasible alternative to study self-heating of biomass [24–27]. This method focuses on assessing the self-heating behavior of a material by analyzing the kinetics involved in the oxidation reaction. However, it is not very clear how to associate the results to a volume, and therefore to a real risk in storage and shipping [15]. A deeper study on the thermal analysis results might therefore help in understanding how to make correspond the results of this test to those obtained with the oven. As a consequence of this, thermal analysis has been used as a reliable screening test before performing the more exhaustive oven test. In the present work, a new approach is tested to enlighten the relations between the oven test and thermal gravimetric analysis. Initially, the self-heating behavior of biochar

pellets with pyrolysis oil as binder are tested by both UN test and thermogravimetric analysis (TGA). By the comparison of results, an experimental campaign is carried out using a thermogravimetric analyzer. To evaluate the complex phenomena affecting the combustion trends of the tested configurations, it has been previously decided to use Response Surface Methodology (RSM) [28]. As suggested in [29], RSM may be useful when the effects of process parameters are not easily distinguishable. This method aims to achieve the best system performance by describing the overall process through a mathematical model [30,31]. In the present work, this statistical model is used in a novel way to evaluate how to produce the biochar/oil pellets to limit the self-heating risk. The aim is to provide further knowledge about how to process biochar pellets blended with pyrolysis oils, in order to avoid self-ignition in the storing and shipping phase. By the knowledge of the authors, no works on this topic are available in literature. Moreover, a new approach to couple thermal analysis and oven test to analyze self-heating is proposed. This solution might facilitate the self-heating assessment of treated biochar pellets with a reduction of costs, easing their potential industrial production and application.

## 2. Material and methods

### 2.1. Feedstock and biochar production

Approximately 5 kg of industrially produced biochar pellets of metallurgical quality were acquired. They were made of softwood pyrolyzed at a temperature between 400 and 600 °C. Before pelletization, the biochar was blended with an industry type pyrolysis oil with a ratio between 20 and 60% of oil. The pellets were then further pyrolyzed in a second heat treatment at the same range of temperatures used in the first pyrolysis. Their average length was about 1.2 cm, as well as the average diameter. Throughout the work, these pellets are named as IBP1. Other biochar pellets were produced in-house, carefully choosing the feedstock and parameters so to have a product with characteristics similar to the provided pellets. A Norway spruce (*Picea abies*) tree was harvested from a local forest in Grimstad, Norway. The tree was felled and chipped. The wood chips were dried at 60 °C for 24 h and then stored in an air-tight tank at ambient temperature. The biochar was generated by the chips in a slow pyrolysis reactor. A modified *SQ 11* top loader furnace (Kittec, Germany) was used for the pyrolysis and a thermo-computer *TC 505* (Bentrup, Germany) was used to control the heating program of the furnace. A Silicon carbide retort was evenly filled up with approximately 100 g of chips and placed inside the furnace. It was then purged with a 40 ml/min nitrogen flow for 15 min before heating, to generate inert atmosphere in the reactor. The feedstock was heated up with a heating rate of 10 °C/min up to the desired temperature. Generally, the pyrolysis temperature used in this work were 450, 600 and 750 °C. The final temperature was kept for 1 h. During the experiment, the nitrogen flow was kept constant. At the end of the session, the feedstock was cooled down to ambient temperature and milled in a hammer mill *px-mfc 90 d* (Polymix, Germany), with a 2 mm sieve. The biochar powders were stored at ambient temperature in airtight boxes. A two stages condensation unit (with set temperature equal to 4 °C) was used to cool down the volatiles and gases leaving the reactor. The non-condensable products were expelled through a chimney. The condensable gases were collected in a quartz glass bottle, cooled down to ambient temperature and stored in air-tight containers at 4 °C, without any further treatment. The second heat treatment was performed at the same range of temperatures used for the pyrolysis and

following the same method. Throughout the work, IBP1 treated at 600 °C is referred as IBPT.

## 2.2. Production of upgraded biochar pellets with pyrolysis oil as binder

Biochar pellets were obtained by using a compact hot single pellet press *EQ-HP-6T* (MTI, USA). Before pelletization, milled biochar was blended with pyrolysis oil at different ratios. For each configuration, the pyrolysis oil produced during the same pyrolysis process which produced the biochar was considered, so to simulate a realistic process chain. As explained in the [supplementary information S1](#), the thermal degradation of pyrolysis oil is not particularly affected by the pyrolysis temperature. The oils produced at different temperatures can therefore be assumed to behave similarly. The blend was mixed, stirred and homogenized in a beaker for approximately 15 min. The pellets die had an inner diameter of 6.25 mm. The amount of mixture fed into the die of the pellet press was carefully regulated for each configuration so to have a maximum pellet length of 4.50 mm. The pelletizing pressure was set by a hydraulic piston to 128 MPa and kept for 10 s before releasing it [32]. Pressure was regulated by a load cell *CPX1000* (Dini Argeo, Italy) connected to a multifunction weight indicator *DFWLB* (Dini Argeo, Italy). The machine components were previously heated up to the operational pelleting temperature of 90 °C. After the extraction, pellets were cooled down to ambient temperature and stored in air-tight containers.

## 2.3. Biochar characterization

Proximate analysis was carried out following the standards EN 14774-2 for the moisture content, EN 15148 for the volatile matter and EN 14775 for the ash content. A *2400 Series II* CHNS/O Elemental Analyzer (PerkinElmer, USA) was used for the C–H–N ultimate analysis. Oxygen was computed by difference with the other elements. Sulphur content was assumed negligible. The higher heating value (HHV) of the biochar was measured in a *C 6000* (IKA calorimeter, Germany) bomb calorimeter. The characterization of the materials which were pelletized is shown in [Table 1](#). A laser diffraction particle size analyzer *Mastersizer 3000* (Malvern, UK) was used to analyze the particle size distribution of the biochar before pelletization. The resulting distributions are presented in [Fig. 1](#). All measurements were conducted in triplicate. The morphology and microstructure of selected materials were examined by a scanning electron microscopy/energy dispersive X-ray Spectroscopy (SEM/EDS) *SU-70* (Hitachi, Japan).

## 2.4. Thermogravimetric analysis

The thermal decomposition was performed by using the

**Table 1**

Proximate analysis, ultimate analysis and high heating value (HHV), with related norms and machine, for the untreated spruce wood and for the spruce biochar produced in house at 450, 600 and 750 °C.

Material	Spruce				Standard	Instrument
	untreated	450	600	750		
Pyrolysis temperature [°C]						
<b>Proximate analysis</b>						LT40/11/P330 (Nabertherm, Germany)
Moisture [%wb]	8.6 ± 0.4	3.2 ± 0.7	5.0 ± 0.6	7.5 ± 0.6	EN 14774-2	
Volatile matter [%db]	80.6 ± 0.3	32.1 ± 0.5	14.6 ± 0.5	9.4 ± 0.3	EN 15148	
Fixed Carbon [%db]	18.6 ± 0.7	62.6 ± 0.7	78.1 ± 0.1	80.7 ± 0.6		
Ash [%db]	0.8 ± 0.3	2.0 ± 0.3	2.3 ± 0.3	2.4 ± 0.2	EN 14775	
<b>Ultimate analysis</b>					EN 16948	2400 Series II CHNS/O Elemental Analyzer (PerkinElmer, USA)
C [%daf]	53.2 ± 0.3	77.8 ± 0.6	89.0 ± 0.5	92.7 ± 0.5		
H [%daf]	6.1 ± 0.2	2.3 ± 0.4	3.1 ± 0.4	2.1 ± 0.3		
N [%daf]	0.1 ± 0.2	3.9 ± 0.2	2.7 ± 0.4	1.7 ± 0.2		
O [%daf]	40.6 ± 0.4	15.8 ± 0.5	5.1 ± 0.2	3.4 ± 0.5		
<b>HHV [MJ/kg, db]</b>	n.a.	29.1 ± 0.3	32.0 ± 0.4	31.9 ± 0.1	EN 14918	Mastersizer 3000 (Malvern, UK)

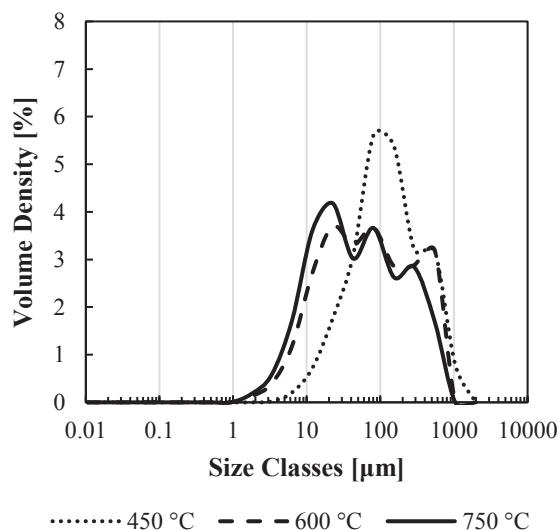


**Fig. 1.** Laser particle size distribution for the biochar produced, before pelletization.

thermogravimetric instrument *TGA/DSC 1 SRTARe System* (Mettler Toledo, USA). The pellet was loaded into a 100 ml  $Al_2O_3$  crucible. It was then heated up to 900 °C at a constant heating rate of 10 °C/min, with a constant dry air volume flow of 50 ml/min. The temperature of initial combustion ( $T_{ic}$ ) and the temperature of maximum weight loss rate ( $T_{mwl}$ ) were directly computed by analyzing the results. The  $T_{ic}$  was considered as the temperature at which the dry weight loss is 1%/min, while the  $T_{mwl}$  as the temperature characterized by the highest weight loss rate, as shown in the example presented in [Fig. 2](#). Some pellets were also treated following the same methodology but substituting the air bottle with argon. The related observations are available in the [Supplementary material S2](#). The activation energy of the reaction was extrapolated by plotting the variation of the specific reaction rate versus the sample temperature, in the range of temperatures where the reaction occurs, under the assumptions and methodology presented in [33].

## 2.5. Statistical model and desirability function

In order to analyze the possible correlations between the biochar pellets production factors and the effects on the self-heating risk behavior, Response Surface Methodology (RSM) with Box-Behnken experimental Design (BBD) was applied. Compared to other common experimental designs, BBD provides generally slightly and significantly higher efficiency [34], and therefore it was selected for this work. BBD

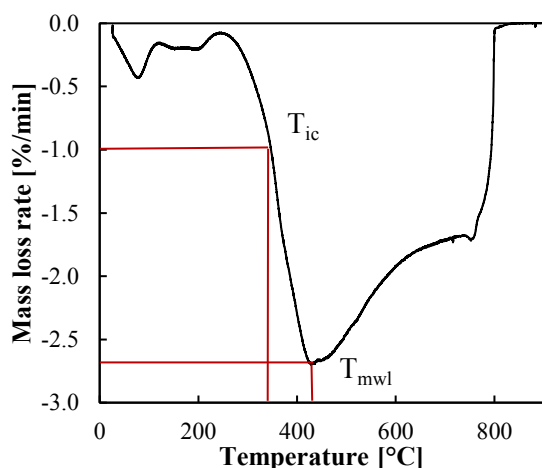


Fig. 2. Differential thermogravimetric (DTG) curve for biochar produced by pyrolysis at 450 °C. The temperature of initial combustion and maximum weight loss are reported.

is a three factors and three levels design, consisting of a replicated center point and a set of points lying at the midpoint of each edge of the multidimensional cube that defines the space of interest. A polynomial quadratic equation was applied to investigate the relationship between the variables and the responses. The independent variables and the associated coded levels that were used in the present work, are presented in Table 2. The pyrolysis temperature ( $X_1$ ), the pyrolysis oil content ( $X_2$ ), and the second heat treatment temperature ( $X_3$ ) were assumed as the independent variables. Each independent variable was prescribed into three levels, coded  $-1$ ,  $0$  and  $+1$ , corresponding to the minimum level, medium level, and maximum level. Each process factor level was carefully selected based on preliminary tests. For the analyzed biochar pellets, the responses were the initial combustion temperature ( $Y_1$ ), the maximum weight loss temperature ( $Y_2$ ) and the activation energy ( $Y_3$ ).

The statistical model was implemented by *Minitab 17.1.0 software* (Minitab Ltd., Coventry, UK). To minimize the bias, 15 runs were selected randomly by the software. They were then carried out, with triplicate center points, in order to estimate the pure error. The combinations of independent variables for each run, together with the observed responses, are shown in Table 3. Analysis of variance (ANOVA) and regression analysis were carried out in order to investigate the statistical significance of the regression coefficients. This was done by performing the Fisher's F-test at 95% confidence level, following the method described in [29]. To better understand how self-heating risks could be minimized, multi-response optimization was applied. The multiple response problem was addressed by using the Derringer's desirability function based approach [35]. The method is described in a more exhaustive way in [13].

## 2.6. Self-heating substances classification test

A specific experiment was designed to test the self-heating behavior of the pellets, according to the classification of the Division 4.2, suggested by the International Maritime Organization (IMO, United Nations) [36]. The test aims at classifying substances in packing groups, which are related to the admissible shipping volumes. In the present work, only the first step was tested, because as shown in Fig. 3, if a new substance passes this step, it is not classified as a self-heating substance of Division 4.2. A stainless-steel cubic basket of 100 mm side with a mesh opening of 0.05 mm was used. The basket sample was housed in a slightly larger cubic container with a mesh opening of 0.60 mm and placed into a modified *SQ 11 top loader furnace* (Kittec, Germany). Air was forced in by an opening placed at one side of the furnace. The

furnace was set up to a temperature of 140 °C which was maintained constant for 24 h. A thermo-computer *TC 505* (Bentrup, Germany) controlled with an application designed on the software *LabVIEW 2019* (National Instrument, USA) was used to regulate the temperatures inside the furnace. The temperatures were measured by four Chromel-Alumel thermocouples (type k). Despite the test requires respectively only one thermocouple, an additional one was used to provide redundancy. The data were collected with a frequency of 1 Hz. If the difference between the temperature of the sample and the temperature of the furnace was exceeding 60 °C (i.e. sample temperature equal to 200 °C), the test was interrupted and considered as not passed. If the threshold temperature difference was not reached within 24 h, the test was considered as passed.

## 3. Results and discussion

### 3.1. Standard test and TGA for industrial biochar pellet

The industrially produced pellets IBP1 were tested with the IMO test. As previously mentioned, these pellets were known not to pass the test. As comparison, another biochar material, which previously passed the test was analyzed. This material was named IBP2 and was provided by the same supplier, which currently uses as Carbon source in a metallurgical application. IBP2 is not pelletized and does not include pyrolysis oil, but it was produced at similar treatment temperatures, in comparison to IBP1. Fig. 4 shows the two different trends for the IMO test performed on IBP1 and IBP2. The results confirmed the initial expectations. The two materials were also compared through a TGA test. Fig. 5 reports the respective normalized mass loss rates per minute. For both materials, a first peak is tracked at around 100 °C, showing water evaporation (water is included into the pyrolysis oil). Secondly, the oxidation phase is distinguished by an evident single peak. Combustion ends with the burn-out of the biochars. Generally the trends are similar to what is observed at the same range of temperatures in [15,37]. According to [38], the characteristic single peak associated to the combustion of biochar is related to the high content of fixed carbon, which makes the material react fast. This behavior is different from the conventional combustion of biomasses, where different peaks are observable and they are linked to the combustion of hemicellulose, cellulose and lignin [20].

For both IBP1 and IBP2,  $T_{ic}$ ,  $T_{mwl}$  and  $E_a$  were computed. The two materials present divergent trends: IPB1 is characterized by high  $E_a$  and low  $T_{ic}$  and  $T_{mwl}$ , while IPB2 has high combustion temperatures and low activation energy. The obtained parameters are listed in Table 4.

Low  $T_{ic}$  and  $T_{mwl}$  are generally associated to a higher predisposition to self-ignition [39]. These value are close to what observed in [38]. For both materials, the activation energy is low, when compared to other tested chars [40,41]. However, in these works, biochar was produced at considerably higher pyrolysis temperatures. Instead, the activation energy values are similar to what observed in [42], where the pyrolysis temperatures were lower. Moreover, by reducing the porosity and reactive surface of the material, the activation energy should generally improve through pelletization [43]. Nevertheless, as observed in [44,45], the computed activation energies of densified biomass might still be very low. Besides, in [46], it was observed that densification

Table 2

Investigated parameters used in the experimental design and their levels (coded and uncoded).

Independent variables	Symbols	Coded levels		
		-1	0	1
Pyrolysis temperature [°C]	X1	450	600	750
Pyrolysis oil content [%]	X2	20	30	40
Second heat treatment temperature[°C]	X3	450	600	750

**Table 3**  
Box-Behnken design and experimental results for each response.

Run order	$X_1$ [°C]	$X_2$ [%]	$X_3$ [°C]	$T_{ic}$ [ $Y_1$ ]		$T_{mwl}$ [ $Y_2$ ]		$E_a$ [ $Y_3$ ]	
				Actual [°C]	Predicted [°C]	Actual [°C]	Predicted [°C]	Actual [kJ/mol]	Predicted [kJ/mol]
1	450	30	450	307.17	309.26	375.50	378.72	21.52	22.16
2	450	20	600	341.50	339.75	402.50	399.07	44.96	45.55
3	450	40	600	336.50	334.74	405.67	403.96	54.38	52.83
4	450	30	750	368.67	368.48	425.33	428.22	37.25	37.22
5	600	20	450	351.33	349.83	420.67	421.43	67.02	65.46
6	600	40	450	346.50	345.23	421.83	420.98	48.19	48.80
7	600	30	600	361.50	357.48	431.00	429.91	70.74	71.17
8	600	30	600	356.50	357.48	428.00	429.91	71.04	71.17
9	600	30	600	355.83	357.48	430.00	429.91	72.20	71.17
10	600	20	750	385.00	385.37	456.67	458.03	67.41	66.47
11	600	40	750	391.17	391.77	468.33	468.08	59.04	60.27
12	750	30	450	379.33	378.61	449.00	446.58	37.16	36.85
13	750	20	600	384.17	385.00	457.17	459.37	68.93	70.13
14	750	40	600	391.00	391.82	460.17	464.08	40.92	39.99
15	750	30	750	404.50	401.47	483.50	480.78	35.25	34.27

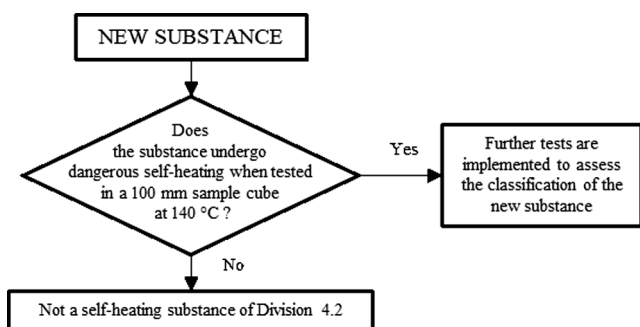


**Fig. 3.** First step of the classification of self-heating substances of Division 4.2, according to IMO (UN) [38], modified.

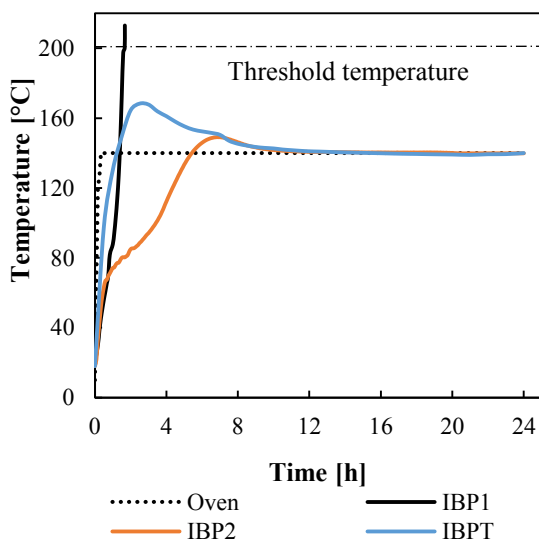


**Fig. 4.** Comparison between IBP1, IBP2 and IBPT in the UN-IMO self-heating test with 10 cm side cube.

tendentially decreases the  $T_{ic}$  and  $T_{mwl}$  of a material, in an extent strictly affected by the type and content of binder. According to the combustion curves presented in Fig. 5, there are instead not evident specific trends that may be directly associated to pyrolysis oil. Also in [45], the addition of coal tar as binder did not affect particularly the characteristics of the combustion. It should be considered that pyrolysis oil included in IBP1 underwent a further pyrolysis at mild temperatures. Hence, that pyrolysis oil partially volatilized and only the

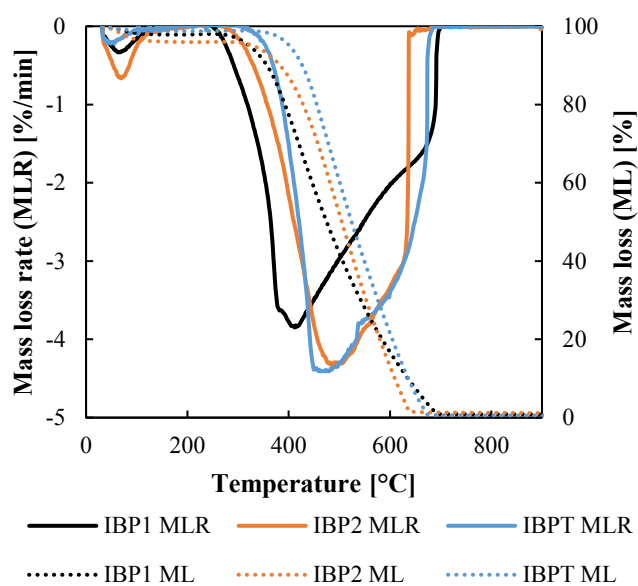


**Fig. 5.** Comparison in TGA between IBP1, IBP2 and IBPT.

**Table 4**  
Temperature of initial combustion ( $T_{ic}$ ), maximum weight loss temperature ( $T_{mwl}$ ) and activation energy ( $E_a$ ) for the materials IBP1, IBP2 and IBPT.

Material	$T_{ic}$ [°C]	$T_{mwl}$ [°C]	$E_a$ [kJ/mol]
IBP1	$308.6 \pm 1.2$	$383.6 \pm 3.6$	$59.6 \pm 2.6$
IBP2	$348.7 \pm 1.5$	$481.5 \pm 2.7$	$38.2 \pm 2.2$
IBPT	$367.3 \pm 2.0$	$459.4 \pm 4.3$	$44.1 \pm 1.8$

carbonized fractions, which resembles char, is therefore present [32]. From the combination of the standardized test and the TGA test, it could hence be inferred that the densification with addition of pyrolysis oil, which brings to a reduction of porosity and surface area during the pelletization phase [13], is the major factor affecting the self-heating behavior of the analyzed pellets. The ratio between volume and external surface increases, resulting in a lower release of the generated heat.

### 3.2. Box-Behnken statistical analysis

The self-heating behavior was then further investigated by the statistical analysis of the produced biochar pellets. In order to evaluate the



effects of pyrolysis temperature ( $X_1$ ), pyrolysis oil content ( $X_2$ ), and second heat treatment temperature ( $X_3$ ) on initial combustion temperature ( $Y_1$ ), maximum weight loss temperature ( $Y_2$ ), and activation energy ( $Y_3$ ), the experimental data shown in Table 3 were subjected to regression analysis. The final predicted process models were obtained as:

$$Y_1 = 246.6 + 0.3069X_1 - 4.92X_2 - 0.0001X_3 + 0.000039X_1X_1 + 0.0447X_2X_2 + 0.000271X_3X_3 + 0.001972X_1X_2 - 0.000404X_1X_3 + 0.001833X_2X_3 \quad (1)$$

$$Y_2 = 293.2 + 0.486X_1 - 3.87X_2 - 0.189X_3 - 0.000152X_1X_1 + 0.0513X_2X_2 + 0.000315X_3X_3 - 0.00003X_1X_2 - 0.000170X_1X_3 + 0.00175X_2X_3$$

$$Y_3 = -665.4 + 1.5687X_1 - 0.451X_2 + 0.8973X_3 - 0.001037X_1X_1 - 0.04294X_2X_2 - 0.000676X_3X_3 - 0.006238X_1X_2 - 0.000196X_1X_3 + 0.001743X_2X_3 \quad (3)$$

The adequacy of the models was analyzed through ANOVA analysis and the results are presented in Table 5. The calculated F-values of 120.83, 84.14, and 166.32 for  $Y_1$ ,  $Y_2$ , and  $Y_3$ , respectively demonstrated that the models were highly significant ( $p \leq 0.001$ ) because there is only a 0.01% chance that these large F-values can occur due to noise. The values of  $R^2$  were 0.9954, 0.9934, 0.9967 for  $Y_1$ ,  $Y_2$ , and  $Y_3$ , showing that only 0.0046%, 0.0066%, and 0.0033% of the total variations were not explained by the regression models. Furthermore, the values of  $R^2_{adj}$  (0.9872, 0.9816, 0.9907) were very high and close to the values of  $R^2$ , confirming that the regression models were highly significant. The acceptability of the quadratic models was also confirmed by the lack of fit (LOF) test which is a measure of the failure of a model to predict data in the experimental domain at which points are not included in the regression. A p-value higher than 0.05 means that LOF is insignificant due to relative pure error. Thus, the lack of fit p-values (0.593, 0.594 and 0.139 for each response) confirms that the models can be effectively employed for the prediction.

### 3.3. Effect of independent variables on the responses

According to the F-values and p-values shown in Table 5, it can be noted that for the initial combustion temperature  $X_1$ ,  $X_3$ ,  $X_2^2$ ,  $X_3^2$ ,  $X_1X_3$  are significant model terms because their p-values were higher than 0.05. The positive sign in the model equation indicates synergistic effects and the negative sign means antagonistic effects on the response. Therefore, from Eq. (1) pyrolysis temperature has a positive effect on the initial combustion temperature, while oil content and second heat treatment have a negative effect. However, the positive sign of quadratic effect of second heat treatment temperature ( $X_3X_3$ ) indicates that initial combustion temperature decreases up to a certain threshold with increasing SHT temperature after which it increases. From the F-values, it can be noted that the pyrolysis temperature had a greater effect on the initial combustion temperature. To investigate the interactive effect of two factors on initial combustion temperature, contour plots were drawn maintaining the third factor at constant level equal to its middle value (i.e.  $X_1$ : 600 °C,  $X_2$ : 30%,  $X_3$ : 600 °C). Fig. 6 shows clearly that the initial combustion temperature increased with increase in pyrolysis and second heat temperatures while the oil content has little influence on this response. In particular, it can be noted that the effect of the oil content is different inside its range of variation because  $T_{in}$  has a minimum when the oil content is equal to 30%. However, as a result of the interactive effects, the maximum value of the response (404.5 °C) was obtained when all three independent variables were at their maximum values.

A similar trend was obtained for the maximum weight loss temperature, for which Eq. (2) shows that linear pyrolysis temperature, linear second heat treatment temperature, and quadratic pyrolysis temperature terms had statistically significant effects on the response.

Eq. (2) is depicted as two-dimensional contour plots in Fig. 7. The highest values of initial combustion temperature were reached at the high levels of pyrolysis temperature and second heat treatment temperature. Oil content seems to show a quadratic behavior where the  $T_{mwl}$  reaches a minimum at approximately 30%. However, an important result from the ANOVA analysis is that the percentage of pyrolysis oil had no significant linear, quadratic and interactive effects on the maximum weight loss temperature.

As regards the activation energy, all linear, quadratic, and interaction terms were significant. In detail, having the highest F-value and regression coefficient, the pyrolysis temperature affected most significantly the activation energy. The oil content, and the second heat treatment temperature also significantly influenced activation energy, even though their influence was lower than that of the pyrolysis temperature. Furthermore, the negative coefficients of the quadratic terms  $X_1^2$  and  $X_2^2$  denoted that there is a possible point of inflexion after which the independent variables have a negative or positive effect on the activation energy. As shown in Fig. 8,  $E_a$  increased with an increase in pyrolysis temperature and second heat treatment temperature both from nearly 450 to 600 °C; nevertheless, beyond 600 °C, activation energy decreased with increasing both temperatures. Fig. 8 shows also that in order to achieve maximum activation energy the oil content should be less than about 33%. Generally, it comes out that responses tend to get maximized when the temperatures of pyrolysis and second heat treatment are high, and the oil content is low.

**Table 5**  
ANOVA of response surface quadratic models.

Source	DF	F-value	Prob > F
<i>Initial combustion temperature</i>			
Model	9	120.83	< 0.0001
$X_1$	1	618.08	< 0.0001
$X_2$	1	0.15	0.717
$X_3$	1	399.77	< 0.0001
$X_1^2$	1	0.34	0.586
$X_2^2$	1	8.65	0.032
$X_3^2$	1	16.09	0.010
$X_1X_2$	1	4.11	0.098
$X_1X_3$	1	38.77	0.002
$X_2X_3$	1	3.55	0.118
Lack of fit	3	0.81	0.593
$R^2 = 0.9954$ . $R^2_{adj} = 0.9872$			
<i>Maximum weight loss temperature</i>			
Model	9	84.14	< 0.0001
$X_1$	1	490.56	< 0.0001
$X_2$	1	3.05	0.141
$X_3$	1	235.40	< 0.0001
$X_1^2$	1	2.92	0.148
$X_2^2$	1	6.56	0.051
$X_3^2$	1	12.53	0.017
$X_1X_2$	1	0.00	0.984
$X_1X_3$	1	3.98	0.103
$X_2X_3$	1	1.86	0.093
Lack of fit	3	9.89	0.594
$R^2 = 0.9934$ . $R^2_{adj} = 0.9816$			
<i>Activation energy</i>			
Model	9	166.32	< 0.0001
$X_1$	1	29.22	0.003
$X_2$	1	105.09	< 0.0001
$X_3$	1	31.55	0.002
$X_1^2$	1	805.82	< 0.0001
$X_2^2$	1	27.31	0.003
$X_3^2$	1	342.64	< 0.0001
$X_1X_2$	1	140.50	< 0.0001
$X_1X_3$	1	31.21	0.003
$X_2X_3$	1	10.97	0.021
Lack of fit	3	6.35	0.139
$R^2 = 0.9967$ . $R^2_{adj} = 0.9907$			

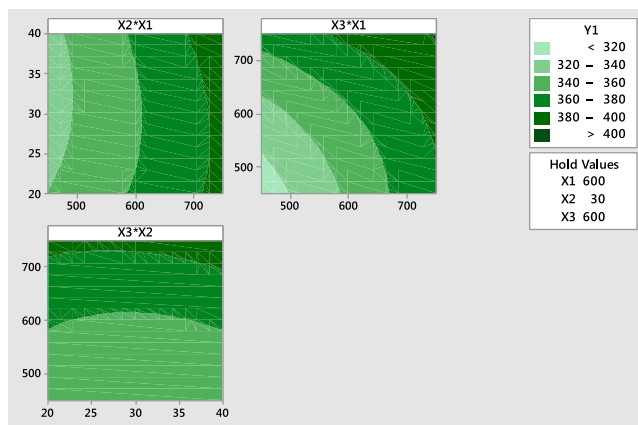


Fig. 6. Contour plots of the initial combustion temperature.

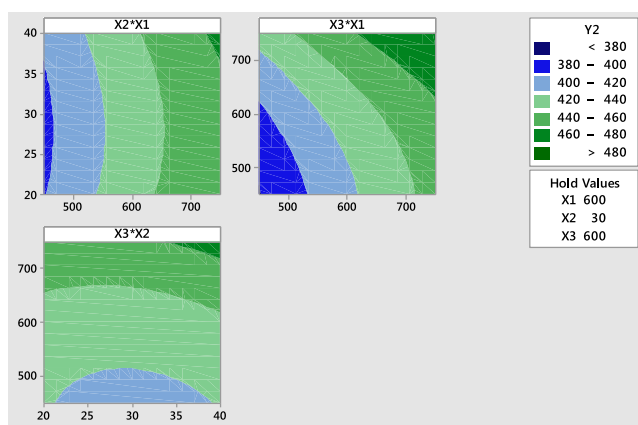


Fig. 7. Contour plots of the maximum weight loss temperature.

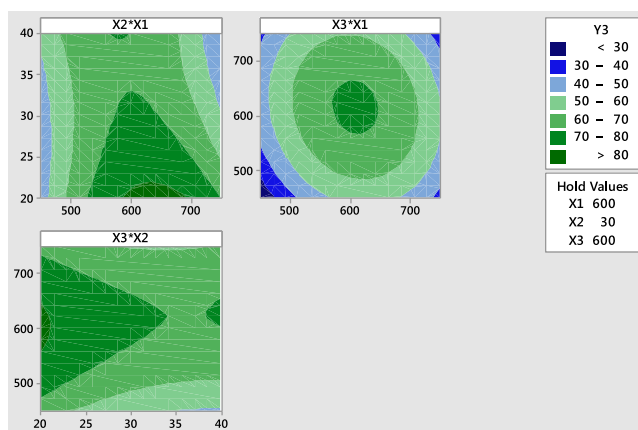


Fig. 8. Contour plots of the activation energy.

### 3.4. Optimization of responses using the desirability function approach

In the production of biochar pellets, high initial combustion temperature, high maximum mass loss rate temperature and high activation energy are desired in order to decrease the self-heating risk. However, the optimization of all responses under the same operative conditions is difficult, because their intervals of variation are different. For this reason, the multi-response optimization for  $T_{in}$ ,  $T_{mwl}$ , and  $E_a$  was carried out by desirability function approach. Composite desirability evaluates how the settings optimize a set of responses overall [29]. In this study, the same weight for all responses and an importance parameter equal to 1 were assumed. As it can be noted from the

Supplementary material Fig. S3, the composite desirability ( $D$ ) of the optimization was 0.8751, that was quite close to the ideal value of 1, which denotes that the chosen optimum settings were in favor of all responses. In particular, the maximum  $T_{in}$ ,  $T_{mwl}$ , and  $E_a$  were found to be 390.2 °C, 467.2 °C, and 68.4 kJ/mol, respectively at an optimal parametric combination of pyrolysis temperature = 698.5 °C, oil content = 20%, and second heat treatment temperature = 716.7 °C.

### 3.5. Discussion over the effects of the independent variables

As support to the statistical analysis, further analyses were taken to consolidate the arisen considerations. Fig. 9 shows the effect of the pyrolysis temperature on the structure of pellets. The differences at different magnitude between pellets produced with biochar at 450 °C (Fig. 9.A-B) and 600 °C (Fig. 9.C-D) are shown. The formers are less compacted, and the particles are tendentially bigger and less porous, as previously shown in Fig. 1. Porous sections are more visible for the biochar produced at 600 °C. Pellets with biochar produced at 450 °C are less compact and less porous and have higher propensity to ignite. The result suggests porosity has a major impact in determining the self-heating behavior, compared to densification, as commented in [47]. Fig. 10 shows instead the impact of using pyrolysis oil as binder. When the binder is included, the reaction starts at lower temperatures and proceeds at a slower pace, without manifesting a rapid oxidation. Pyrolysis oil covers the pores, limiting the transfer of heat. Therefore, the material will be heated up and get ignited faster. The oxidation then will proceed slower since less surface is available. As confirmation, when the specific exothermic energy was computed, both curves have similar results (ca. 10 kJ/kg). Once the pellets are newly treated with re-heating, the porosity increases and the ratio between volume and external surfaces decreases, with direct benefit in terms of higher heat losses. This is clearly shown in Fig. 11. Pellets with biochar produced at 450 °C present a more compact and porous structure, when treated at 600 °C (Fig. 11.A), in comparison to Fig. 9.B. Fig. 11.B-D show instead that a fraction of the pyrolysis oil got volatilized and parts of it are carbonized in the newly open porous surface.

### 3.6. Analysis of the treated industrial pellets

According to the results obtained by the statistical analysis, the industrial pellets IBP1 were further treated by a second heat treatment at 600 °C (IBPT). The idea was to intervene on the pellets, to possibly increase the responses. IBPT was then further analyzed by TGA. The normalized mass loss rate per minute is shown in Fig. 5, in comparison to IBP1 and IBP2. Once treated, IBPT differ from IBP1, approaching the trend observed with IBP2. Both  $T_{ic}$  and  $T_{mw}$  increased up to  $367.3 \pm 2.0$  °C and  $459.4 \pm 4.3$  °C, respectively. Instead, the activation energy  $E_a$  decreased to  $44.1 \pm 1.8$  kJ/mol. These values are compared to what obtained with IBP1 and IBP2 in Table 4. Despite that the statistical results showed a correlation between the increase of  $E_a$  and the increase of second heat treatment temperature, IBPT is characterized by a lower activation energy than IBP1. However, if the contour plot in Fig. 8, showing the effect on the activation energy of the binder and the second heat treatment, is considered, it can be noticed that easily distinguishable patterns are not present. It is therefore complex to predict the behavior outside the selected range of binder content. The oils used in IBP1 were produced by an optimized industrial process, and they might therefore present a lower water content compared to the lab-produced pyrolysis oils. At fixed weight, the former ones might have a higher organic compounds content. The actual oil content in IBPT could therefore lay outside the selected range, and above 40%. As observed in [13], oil as binder tends to provide negative effects on pellet quality when the content is too high. This result implies that the influence of pyrolysis oil on the activation energy represents an interesting topic for further works. However, if IBPT is compared to IBP2, which is considered no self-heating risk material, values of  $T_{ic}$

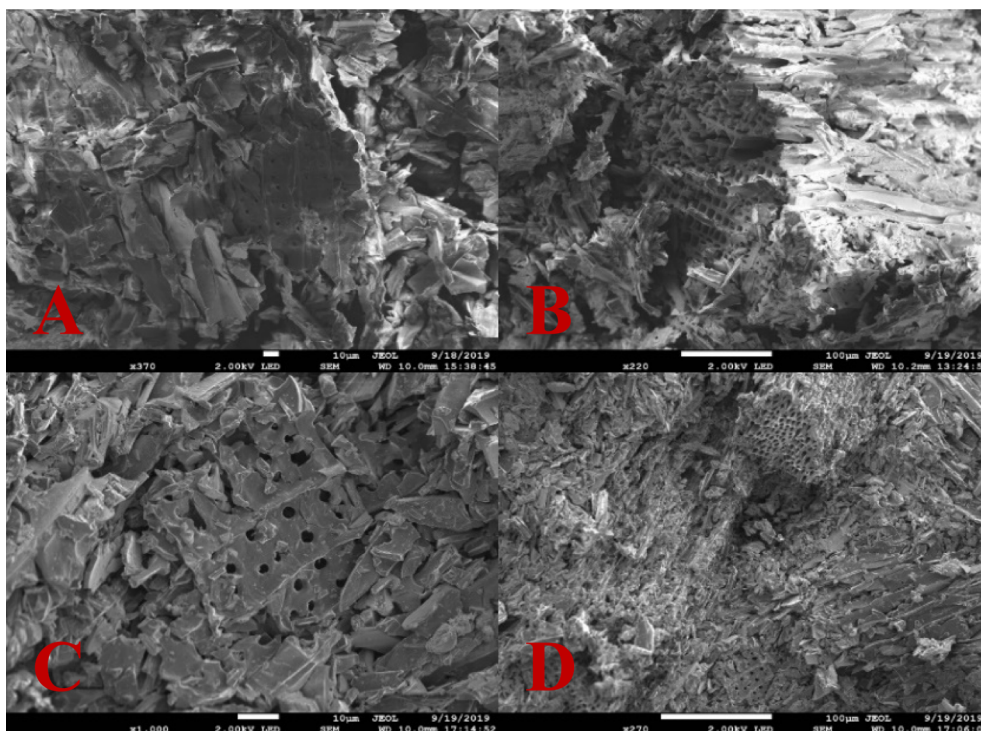


Fig. 9. Scanning electron microscope (SEM) photos for: biochar produced at 450 °C, blended with 30% (A) and 20% (B) of pyrolysis oil; biochar produced at 600 °C, blended with 30% of pyrolysis oil (C-D).

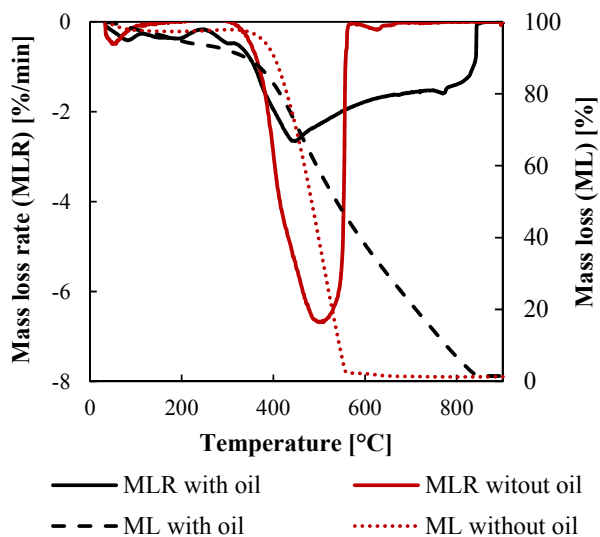


Fig. 10. Comparison in TGA between pellet with biochar produced at 600 °C, with and without pyrolysis oil as binder (30%).

differ of +5.1%, values of  $T_{mwl}$  differ of -4.9% and values of  $E_a$  differ of -13.6%. This suggests a low predisposition for self-heating. As previously observed, when pyrolysis oil is used as binder, a further pyrolysis treatment enables the partial volatilization of it, with a consequent increase of porosity and surface area. The material can hence dissipate heat faster, delaying the oxidation process and the risk of self-heating. IBPT was also tested by IMO procedure. The result is presented in Fig. 4. After the treatment, the material can successfully pass the test and it is not classified as self-heated material. Such result leads to some important considerations. When pyrolysis oil is used as binder, a second heat treatment at high temperatures is highly recommended, since the self-heating risk drastically drops. Considering that the coupling of oil and treatment was also observed to be associated to a strong

improvements in mechanical properties [13,32], this result offers a further confirmation of the utility of processing a second heat treatment for this kind of biochar pellets. The direct cost related to the inclusion of a further heat treatment, might be balanced by evident benefits both in the application and in the transportation and storage of biochar pellets. Moreover, according to the results,  $T_{ic}$  and  $T_{mwl}$  may be key factors associated to self-heating behavior, while the relation to activation energy is less clear. The results legitimated the TGA as a useful screening test before performing the standardized tests for biochar, with a consequent reduction in research and development (R&D) costs. This possibility was hinted in [15], but not clearly showed.

### 3.7. $E_a$ vs. $T_{mwl}$ graph for self-heating risk evaluation

A graph, including the values of  $E_a$  and  $T_{mwl}$  for all the configurations analyzed in this work, was built and it is presented in Fig. 12. This graph was used upon the idea of simplifying what has been discussed so far and defining an easily usable and interpretable criterium to assess the self-heating risk of biochar pellets. In [27], a similar diagram was presented and different categories of risk were listed, according to values obtained from several types of coal and biomass. These materials are characterized by lower values of  $E_a$  and  $T_{mwl}$  than those analyzed in the present work. According to [27], the self-heating risk decreases at higher  $T_{mwl}$ . The graph must therefore be adjusted accordingly. This was done, for example, in [25], where new areas or risk were suggested. Similar considerations were used in [48]. None of these works studied either biochar or densified materials. Hence, according to the assumptions which were drawn in the mentioned literature, a new risk graph was built up. The aim is to adjust the diagram to make it suitable to assess the self-heating behavior of biochar pellets. The graph in Fig. 12 locates materials in different areas of risk, considering their values of  $E_a$  and  $T_{mwl}$ . The areas or risk are divided in: very high, high, low, very low; according to the tendency pellets had to self-ignite in the oven test. In particular:

- the very high risk and high risk areas are traced considering the



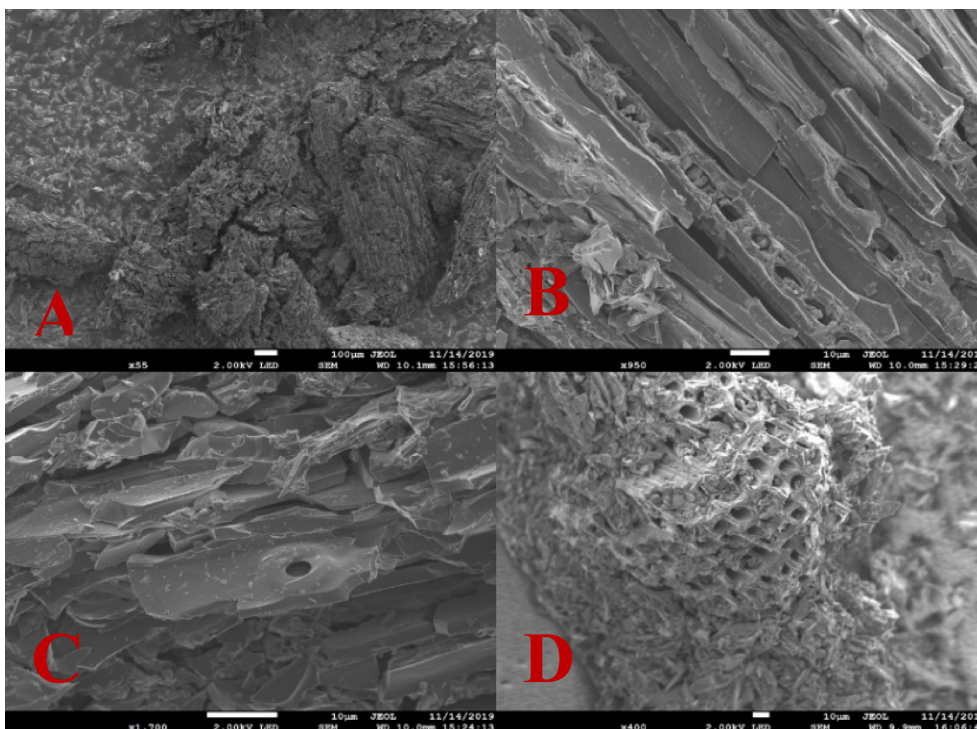


Fig. 11. Scanning electron microscope (SEM) photos for: biochar produced at 450 °C, blended with 30% of pyrolysis oil, treated at 600C (A); biochar produced at 600 °C, blended with 30% of pyrolysis oil, treated at 600 °C (B-C); biochar produced at 750 °C, blended with 30% of pyrolysis oil, treated at 750 °C (D).

values of  $E_a$  and  $T_{mwl}$  of two selected materials. The high risk area is limited by the values obtained from the TGA of IBP1. The very high risk region was instead built according to the tests carried out with a further provided material labelled as IBP3. This material was industrially produced in the same way of IBP1 by the same provider, with the addition of a further curing treatment. From preliminary studies, IBP3 provided the highest tendency to ignite.

- The low and very low risk areas are marked considering exclusively the  $T_{mwl}$ , because its effect on self-heating behavior is considered predominant over  $E_a$ . The low risk and the very low risk areas are limited by IBP2 and IBPT, respectively.
- Between the high risk and the low risk areas, the findings were not

enough to predict successfully the oven test response. This zone is therefore considered as an uncertainty area, where TGA cannot detect precisely the outcome of the oven test.

IBP1, IBP2, IBP3 and IBPBT were used as benchmark since their inclination to self-heating was assessed by standardized tests. Moreover, as they are currently produced industrially, they might provide relevant information, once other materials are analyzed. According to Fig. 12, some considerations can be extracted. Pellets including biochar produced at 450 °C must undergo a second heat treatment at least at 600 °C to move outside the high risk area. At the same time, even if treated at 600 °C, the pellets with biochar produced

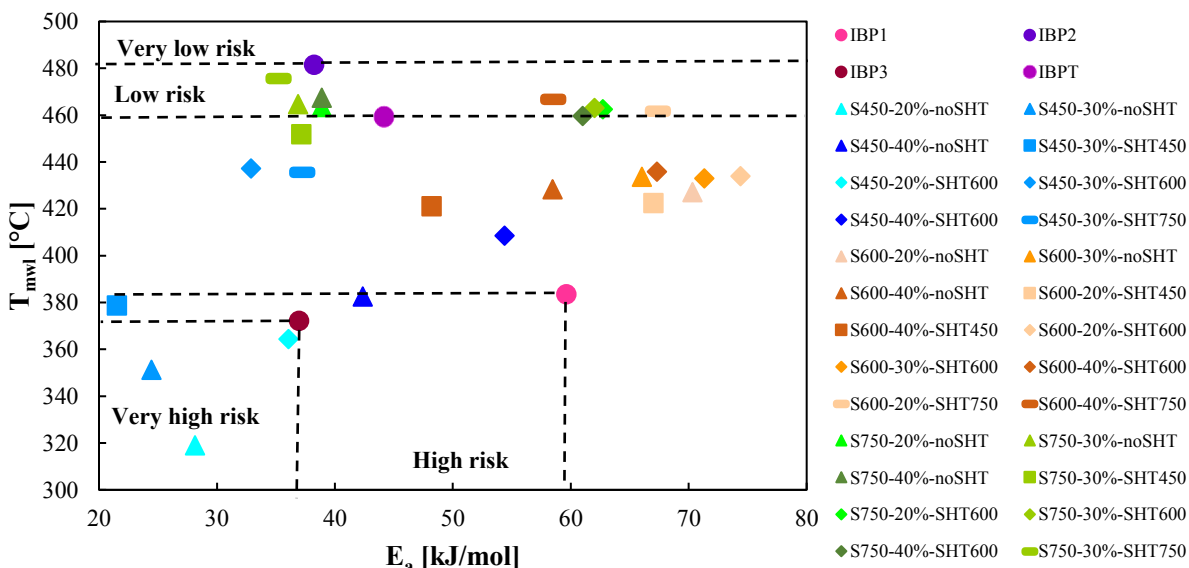


Fig. 12. Activation energy ( $E_a$ ) vs Maximum weight loss temperature ( $T_{mwl}$ ) graph, associated to suggested risk areas based upon all the configurations analyzed throughout this work.

at 450 °C and with 20% of pyrolysis oil as binder have high self-heating risk. It is possible that the oil content was not enough to affect significantly the structure of the pellets. The porosity of the re-heated biochar pellets is therefore yet similar to the untreated biochar. When biochar was produced at 600 or 750 °C, the risk is tendentially lower. In this case, it can be observed that all the combinations, having at least either pyrolysis or second heat treatment carried at 750 °C, are placed in the nearby of the suggested low risk line. These results confirm the importance of processing the heating treatments at high temperatures, so to limit the tendency of pellets to self-ignite. The effect of pyrolysis oil as binder varies according to the initial pyrolysis temperature. For high pyrolysis temperatures, an increase of oil content leads to a decrease of activation energy, without having an observable impact on the maximum weight loss temperature. When the pyrolysis temperature is 450 °C, the effect of the oil content is less clear and should be addressed in further works. These results may be useful to adjust the process parameters of pellets production, according to their possible place in the graph.

#### 4. Conclusions

The statistical analysis permitted to identify the main variables, which affect the self-heating behavior of upgraded biochar pellets blended with pyrolysis oil. It was found out that it is possible to intervene on the self-heating behavior of biochar pellets by choosing carefully the temperatures in pyrolysis and in the second heat treatment. Upgraded biochar pellets present a lower self-heating risk, if one of the heat treatments is processed at least at 600 °C. The findings were then further validated by a standardized self-heating test. It was observed that pellets, which previously did not pass the test, could successfully pass it, once re-heated at 600 °C. The result legitimates the analysis and observations obtained by the thermogravimetric experiments, as a valid and useful feedback to understand how a material may react in the standardized test. In this peculiar case, the TGA tests helped in rapidly finding a solution about an existing problem experienced at an industrial scale. This work is therefore intended to show two novel and important findings:

- biochar pellets blended with pyrolysis oil have been previously demonstrated to offer good quality in terms of mechanical properties. However, the use of pyrolysis oil as binder it is associated to an increase of risk of self-ignition. In the present work, it was observed that the self-ignition behavior of biochar pellets blended with pyrolysis oil is strongly affected by the pyrolysis temperature and it is possible to decrease the risk of self-ignition by newly thermally treating the pellets with a further pyrolysis at high temperatures.
- TGA can provide important information about the self-heating behavior of biochar pellets, and in general of a material. This option is strictly related to a reduction of costs in terms of time and material, enabling the possibility of testing a more extended set of configurations both at a research and industrial scale.

Moreover, a risk tendency graph was built upon the obtained results. This graph is not intended to be exhaustive and complete but can potentially support further developments on industrial use of biochar pellets.

#### CRedit authorship contribution statement

**Lorenzo Riva:** Conceptualization, Methodology, Software, Validation, Investigation, Data curation, Writing - original draft. **Alessandro Cardarelli:** Validation, Investigation, Software, Data curation, Writing - original draft. **Geir Johan Andersen:** Conceptualization, Resources, Methodology. **Therese Videm Buø:** Conceptualization, Resources, Methodology. **Marco Barbanera:** Visualization, Software, Formal analysis, Writing - original draft. **Pietro**

**Bartocci:** Data curation, Supervision, Writing - review & editing. **Francesco Fantozzi:** Supervision, Resources. **Henrik Kofoed Nielsen:** Supervision, Resources, Writing - review & editing.

#### Declaration of Competing Interest

The authors declare that they have no known competing financial interests or personal relationships that could have appeared to influence the work reported in this paper.

#### Acknowledgments

This research did not receive any specific grant from funding agencies in the public, commercial, or not-for-profit sectors. The authors acknowledge Naureen Akhtar (University of Agder) for the assistance provided for the scanning electron microscope, as well as Johan Olav Brakestad, Steve Schading and Gerrit Ralf Surup (University of Agder) for the support in setting up the experimental set up.

#### Appendix A. Supplementary data

Supplementary data to this article can be found online at <https://doi.org/10.1016/j.fuel.2020.118395>.

#### References

- [1] Lee M, Lin Y-L, Chiueh P-T, Den W. Environmental and energy assessment of biomass residues to biochar as fuel: A brief review with recommendations for future bioenergy systems. *J Clean Prod Apr.* 2020;251:119714 <https://doi.org/10.1016/j.jclepro.2019.119714>.
- [2] Dufourny A, Van De Steene L, Humbert G, Guibal D, Martin L, Blin J. Influence of pyrolysis conditions and the nature of the wood on the quality of charcoal as a reducing agent. *J Anal Appl Pyrolysis* 2019;137:1–13. <https://doi.org/10.1016/j.jaap.2018.10.013>.
- [3] Griessacher T, Antrekowitsch J, Steinlechner S. Charcoal from agricultural residues as alternative reducing agent in metal recycling. *Biomass Bioenergy* 2012;39:139–46. <https://doi.org/10.1016/j.biombioe.2011.12.043>.
- [4] Meier T, et al. Process modeling and simulation of biochar usage in an electric arc furnace as a substitute for fossil coal. *Steel Res Int* 2017;88(9):1600458. <https://doi.org/10.1002/srin.201600458>.
- [5] Monsen B, Lindstad T, Tuset JK. CO<sub>2</sub> emissions from the production of ferrosilicon and silicon metal in Norway. *56th Electric furnace conference proceedings, New Orleans, USA.* 1998. p. 371–8.
- [6] Demus T, Reichel T, Schulten M, Echterhof T, Pfeifer H. Increasing the sustainability of steel production in the electric arc furnace by substituting fossil coal with biochar agglomerates. *Ironmak. Steelmak.* 2016;43(8):564–70. <https://doi.org/10.1080/03019233.2016.1168564>.
- [7] Surup GR, et al. Effect of operating conditions and feedstock composition on the properties of manganese oxide or quartz charcoal pellets for the use in ferroalloy industries. *Energy* 2020;193:116736 <https://doi.org/10.1016/j.energy.2019.116736>.
- [8] Monsen B, Tangstad M, Midtgaard H. Use of charcoal in silicomanganese production. *Tenth International Ferroalloys Congress, Cape Town, South Africa.* 2004. p. 392–404.
- [9] Wang L, Buvarp F, Skreiberg Ø, Bartocci P. A study on densification and CO<sub>2</sub> gasification of biocarbon. *Chem Eng Trans, Bologna, Italy* 2018;65:145–50.
- [10] Bazargan A, Rough SL, McKay G. Compaction of palm kernel shell biochars for application as solid fuel. *Biomass Bioenergy* 2014;70:489–97. <https://doi.org/10.1016/j.biombioe.2014.08.015>.
- [11] Riva L, Surup GR, Buø TV, Nielsen HK. A study of densified biochar as carbon source in the silicon and ferrosilicon production. *Energy Aug.* 2019;181:985–96. <https://doi.org/10.1016/j.energy.2019.06.013>.
- [12] Monsen B, Gronli M, Nygaard L, Tveit H. "The use of biocarbon in Norwegian ferroalloy production," presented at the INFACON 9, Quebec City, Canada, 2001, pp. 268–76.
- [13] Riva L, et al. Analysis of optimal temperature, pressure and binder quantity for the production of biocarbon pellet to be used as a substitute for coke. *Appl Energy* 2019;256:113933 <https://doi.org/10.1016/j.apenergy.2019.113933>.
- [14] Drysdale D. *An introduction to fire dynamics.* Chichester, UK: John Wiley & Sons Ltd; 2011.
- [15] Restuccia F, Mašek O, Hadden RM, Rein G. Quantifying self-heating ignition of biochar as a function of feedstock and the pyrolysis reactor temperature. *Fuel* 2019;236:201–13. <https://doi.org/10.1016/j.fuel.2018.08.141>.
- [16] Bustos-Vanegas JD, Martins MA, Freitas AG, Mellmann J. Experimental characterization of self-heating behavior of charcoal from eucalyptus wood. *Fuel* 2019;244:412–8. <https://doi.org/10.1016/j.fuel.2019.01.136>.
- [17] Evangelista B, Arlabosse P, Govin A, Salvador S, Bonnefoy O, Dirion J-L. Reactor

- scale study of self-heating and self-ignition of torrefied wood in contact with oxygen. *Fuel* 2018;214:590–6. <https://doi.org/10.1016/j.fuel.2017.11.048>.
- [18] Restuccia F, Ptak N, Rein G. Self-heating behavior and ignition of shale rock. *Combust Flame* 2017;176:213–9. <https://doi.org/10.1016/j.combustflame.2016.09.025>.
- [19] Restuccia F, Huang X, Rein G. Self-ignition of natural fuels: Can wildfires of carbon-rich soil start by self-heating? *Fire Saf J* 2017;91:828–34. <https://doi.org/10.1016/j.firesaf.2017.03.052>.
- [20] García-Torrent J, Ramírez-Gómez Á, Querol-Aragón E, Grima-Olmedo C, Medic-Pejic L. Determination of the risk of self-ignition of coals and biomass materials. *J Hazard Mater* 2012;213–214:230–5. <https://doi.org/10.1016/j.jhazmat.2012.01.086>.
- [21] Zhao MY, Enders A, Lehmann J. Short- and long-term flammability of biochars. *Biomass Bioenergy* 2014;69:183–91. <https://doi.org/10.1016/j.biombioe.2014.07.017>.
- [22] Bilbao R, Mastral JF, Aldea ME, Ceamanos J, Betrán M, Lana JA. Experimental and theoretical study of the ignition and smoldering of wood including convective effects. *Combust Flame* 2001;126(1–2):1363–72. [https://doi.org/10.1016/S0010-2180\(01\)00251-6](https://doi.org/10.1016/S0010-2180(01)00251-6).
- [23] van Blijderveen M, Gucho EM, Bramer EA, Brem G. Spontaneous ignition of wood, char and RDF in a lab scale packed bed. *Fuel* 2010;89(9):2393–404. <https://doi.org/10.1016/j.fuel.2010.01.021>.
- [24] Grotkjær T, Dam-Johansen K, Jensen AD, Glarborg P. An experimental study of biomass ignition. *Fuel* 2003;82(7):825–33. [https://doi.org/10.1016/S0016-2361\(02\)00369-1](https://doi.org/10.1016/S0016-2361(02)00369-1).
- [25] Jones JM, et al. Low temperature ignition of biomass. *Fuel Process Technol* 2015;134:372–7. <https://doi.org/10.1016/j.fuproc.2015.02.019>.
- [26] Rousset P, Mondher B, Candellier K, Volle G, Dibdiakova J, Humbert G. Comparing four bio-reducers self-ignition propensity by applying heat-based methods derived from coal. *Thermochim Acta* 2017;655:13–20. <https://doi.org/10.1016/j.tca.2017.06.006>.
- [27] Garcia Torrent J, Fernandez Anez N, Medic Pejic L, Montenegro Mateos L. Assessment of self-ignition risks of solid biofuels by thermal analysis. *Fuel* 2015;143:484–91. <https://doi.org/10.1016/j.fuel.2014.11.074>.
- [28] Myers RH, Montgomery DC, Anderson-Cook CM. *Response surface methodology: process and product optimization using designed experiments*. Fourth edition Hoboken, New Jersey: Wiley; 2016.
- [29] Buratti C, Barbanera M, Lascano E, Cotana F. Optimization of torrefaction conditions of coffee industry residues using desirability function approach. *Waste Manag* 2018;73:523–34. <https://doi.org/10.1016/j.wasman.2017.04.012>.
- [30] Prakash Maran J, Manikandan S. Response surface modeling and optimization of process parameters for aqueous extraction of pigments from prickly pear (*Opuntia ficus-indica*) fruit. *Dyes Pigments* 2012;95(3):465–72. <https://doi.org/10.1016/j.dyepig.2012.06.007>.
- [31] Qiang H, Wang F, Ding J, Zhang C. Co-digestion of swine manure and corn stalks with biochar as an effective promoter: an optimization study using response surface methodology. *Fuel* 2020;268:117395 <https://doi.org/10.1016/j.fuel.2020.117395>.
- [32] Riva L, Surup GR, Buø TV, Nielsen HK. A study on densified biochar as carbon source in the silicon and ferrosilicon production, Manuscript submitted for publication 2019.
- [33] Cumming JW. Reactivity assessment of coals via a weighted mean activation energy. *Fuel* 1984;63(10):1436–40. [https://doi.org/10.1016/0016-2361\(84\)90353-3](https://doi.org/10.1016/0016-2361(84)90353-3).
- [34] Ferreira SLC, et al. Box-Behnken design: An alternative for the optimization of analytical methods. *Anal Chim Acta* 2007;597(2):179–86. <https://doi.org/10.1016/j.aca.2007.07.011>.
- [35] Derringer G, Suich R. Simultaneous Optimization of Several Response Variables. *J Qual Technol* 1980;12(4):214–9. <https://doi.org/10.1080/00224065.1980.11980968>.
- [36] United Nationseditor. *Recommendations on the transport of dangerous goods: model regulations*. New York: United Nations; 2009.
- [37] Yi Q, et al. Thermogravimetric analysis of co-combustion of biomass and biochar. *J Therm Anal Calorim* 2013;112(3):1475–9. <https://doi.org/10.1007/s10973-012-2744-1>.
- [38] Mau V, Gross A. Energy conversion and gas emissions from production and combustion of poultry-litter-derived hydrochar and biochar. *Appl Energy* 2018;213:510–9. <https://doi.org/10.1016/j.apenergy.2017.11.033>.
- [39] Lu J-J, Chen W-H. Investigation on the ignition and burnout temperatures of bamboo and sugarcane bagasse by thermogravimetric analysis. *Appl Energy* 2015;160:49–57. <https://doi.org/10.1016/j.apenergy.2015.09.026>.
- [40] Kastanaki E, Vamvuka D. A comparative reactivity and kinetic study on the combustion of coal-biomass char blends. *Fuel* 2006;85(9):1186–93. <https://doi.org/10.1016/j.fuel.2005.11.004>.
- [41] Gil MV, Casal D, Pevida C, Pis JJ, Rubiera F. Thermal behaviour and kinetics of coal/biomass blends during co-combustion. *Bioresour Technol* 2010;101(14):5601–8. <https://doi.org/10.1016/j.biortech.2010.02.008>.
- [42] Toptas A, Yildirim Y, Duman G, Yanik J. Combustion behavior of different kinds of torrefied biomass and their blends with lignite. *Bioresour Technol* 2015;177:328–36. <https://doi.org/10.1016/j.biortech.2014.11.072>.
- [43] Gangil S. Beneficial transitions in thermogravimetric signals and activation energy levels due to briquetting of raw pigeon pea stalk. *Fuel Jul.* 2014;128:7–13. <https://doi.org/10.1016/j.fuel.2014.02.065>.
- [44] Onsrée T, Tippayawong N, Zheng A, Li H. Pyrolysis behavior and kinetics of corn residue pellets and eucalyptus wood chips in a macro thermogravimetric analyzer. *Case Stud Therm Eng* 2018;12:546–56. <https://doi.org/10.1016/j.csite.2018.07.011>.
- [45] Cheng J, Zhou F, Si T, Zhou J, Cen K. Mechanical strength and combustion properties of biomass pellets prepared with coal tar residue as a binder. *Fuel Process Technol* 2018;179:229–37. <https://doi.org/10.1016/j.fuproc.2018.07.011>.
- [46] Hu Q, Shao J, Yang H, Yao D, Wang X, Chen H. Effects of binders on the properties of bio-char pellets. *Appl Energy* 2015;157:508–16. <https://doi.org/10.1016/j.apenergy.2015.05.019>.
- [47] Cruz Ceballos DC, Hawboldt K, Helleur R. Effect of production conditions on self-heating propensity of torrefied sawmill residues. *Fuel* 2015;160:227–37. <https://doi.org/10.1016/j.fuel.2015.07.097>.
- [48] Ramírez A, García-Torrent J, Tascón A. Experimental determination of self-heating and self-ignition risks associated with the dusts of agricultural materials commonly stored in silos. *J Hazard Mater* 2010;175(1–3):920–7. <https://doi.org/10.1016/j.jhazmat.2009.10.096>.